Antivascular and antitumor evaluation of 2-amino-4-(3-bromo-4, 5-dimethoxy-phenyl)-3-cyano-4*H*-chromenes, a novel series of anticancer agents

Henriette Gourdeau,[1] Lorraine Leblond,[1]
Bettina Hamelin,[1] Clemence Desputeau,[1]
Kelly Dong,[1] Irenej Kianicka,[1] Dominique Custeau,[1]
Chantal Boudreau,[1] Lilianne Geerts,[1]
Sui-Xiong Cai,[2] John Drewe,[2] Denis Labrecque,[1]
Shailaja Kasibhatla,[2] and Ben Tseng[2]

[1]Shire BioChem, Inc., Laval, Quebec, Canada and [2]Maxim Pharmaceuticals, Inc., San Diego, California

Abstract

A novel series of 2-amino-4-(3-bromo-4,5-dimethoxy-phenyl)-3-cyano-4*H*-chromenes was identified as potent apoptosis inducers through a cell-based high throughput screening assay. Six compounds from this series, MX-58151, MX-58276, MX-76747, MX-116214, MX-116407, and MX-126303, were further profiled and shown to have potent *in vitro* cytotoxic activity toward proliferating cells only and to interact with tubulin at the colchicine-binding site, thereby inhibiting tubulin polymerization and leading to cell cycle arrest and apoptosis. Furthermore, these compounds were shown to disrupt newly formed capillary tubes *in vitro* at low nanomolar concentrations. These data suggested that the compounds might have vascular targeting activity. In this study, we have evaluated the ability of these compounds to disrupt tumor vasculature and to induce tumor necrosis. We investigated the pharmacokinetic and toxicity profiles of all six compounds and examined their ability to induce tumor necrosis. We next examined the antitumor efficacy of a subset of compounds in three different human solid tumor xenografts. In the human lung tumor xenograft (Calu-6), MX-116407 was highly active, producing tumor regressions in all 10 animals. Moreover, MX-116407 significantly enhanced the antitumor activity of cisplatin, resulting in 40% tumor-free animals at time of sacrifice. Our results identify MX-116407 as the lead candidate and strongly support its continued development as a novel anticancer agent for human use. [Mol Cancer Ther 2004;3(11):1375–83]

Introduction

The initial hit compound of a novel series of 2-amino-4-(3-bromo-4,5-dimethoxy-phenyl)-3-cyano-4*H*-chromenes was identified in a cell-based high throughput screening assay by measuring the induction of apoptosis using our pro-fluorescent caspase substrate (1–3). Analogues were made of the hit compound and activity and stability optimization studies identified six analogues synthesized in this series (MX-58151, MX-58276, MX-76747, MX-116214, MX-116407, and MX-126303) for further characterization. Compounds from this series were shown to have potent *in vitro* cytotoxic activity toward proliferating cells only and to interact with tubulin at the colchicine-binding site, thereby inhibiting tubulin polymerization and leading to cell cycle arrest and apoptosis (4). Furthermore, these compounds were shown to disrupt newly formed capillary tubes *in vitro* at low nanomolar concentrations. This activity suggested that the compounds might have vascular targeting activity.

Microtubules are highly dynamic assemblies of the protein tubulin and are major structural components in cells. They are important in the maintenance of cell shape, cellular movement, and cell division (5–7). Tubulin represents one of the best cancer targets identified to date given the large and diverse group of tubulin targeting anticancer drugs and their success in the clinic (8–12). These drugs, by interfering with the dynamic instability of tubulin, arrest dividing cells in the M phase of the cell cycle leading to apoptotic cell death. However, emerging resistance to antimitotic agents has limited their ultimate effectiveness and there is a renewed interest in the discovery and development of new agents that are active in multidrug-resistant cells and that interact with tubulin at sites different from those of the taxanes and *Vinca* alkaloids (13). This field has exploded in the last few years and led to the discovery of small molecular weight inhibitors that have shown promising antitumor activity even in tumors expressing multidrug-resistant phenotypes (14).

In addition to their tubulin-mediated cytotoxicity, *Vinca* alkaloids and colchicine have also been reported to induce hemorrhagic necrosis of solid tumors (15). However, because these additive antitumor effects were only observed at doses approaching or exceeding their maximum tolerated dose (MTD), this attribute has not been fully explored. This has led to the development of a second generation of tubulin-binding agents that destabilize the tubulin cytoskeleton by interacting at the colchicine-binding site at doses that are well tolerated (16). Due to their short half-lives, these compounds preferentially target tumor endothelial cells while sparing normal vasculature (17, 18). These agents, exemplified by combretastatin A-4

phosphate (CA4P) prodrug and ZD6126, both of which are analogues of colchicines, are called vascular targeting agents. Unlike antiangiogenesis drugs, which attempt to prevent the formation of new tumor blood vessels, vascular targeting agents starve existing solid tumors by depriving them of blood flow, causing tumor cell death.

In this study, we have evaluated the ability of 2-amino-4-(3-bromo-4,5-dimethoxy-phenyl)-3-cyano-4*H*-chromenes compounds to induce tumor necrosis and their potential to act as antitumor agents. To this end, we investigated the pharmacokinetic and toxicity profiles of these six compounds in the series and examined their ability to induce tumor necrosis. We also examined the antitumor efficacy of a subset of these compounds in three different human solid tumor xenografts and addressed the chemoenhancing potential of the optimal analogue.

Materials and Methods

Compounds

ZD6126 was synthesized at Shire BioChem (Laval, Quebec, Canada) according to published procedures (19). MX-58151, MX-58276, MX-76747, MX-116214, MX-116407, and MX-126303 were synthesized at Shire BioChem and Maxim Pharmaceuticals according to methods described previously (4).[3] MX compounds were dissolved in a mixture of Cremophor EL (5-10%) and ethanol (5-10%) in saline; ZD6126 was dissolved in water and 5% aqueous sodium carbonate solution was added drop-wise until a clear solution was obtained; cisplatin (0.4 mg/mL) was dissolved in 0.9% saline. Drugs were given at constant injection volumes of 10 mL/kg of mouse body weight i.p. (ZD6126 and cisplatin) or i.v. (MX compounds).

Cell Culture

The human lung carcinoma Calu-6 cell line was purchased from the American Type Culture Collection (Manassas, VA); the human breast carcinoma MDA-MB-435 cell line was obtained from the Frederick Research Tumor Repository (Frederick, MD). Cell lines were maintained in either MEM (Calu-6) or RPMI 1640 (MDA-MB-435) supplemented with fetal bovine serum (10%, Life Technologies, Burlington, Ontario, Canada) and supplements (nonessential amino acids, glutamine, sodium pyruvate, vitamins, and glucose; Cellgro Mediatech, Inc., Herndon, VA) according to the cell supplier's instructions. All cell lines were maintained at 37°C in a humidified atmosphere of 95% air and 5% CO_2. Cells were grown in absence of antibiotics and periodically checked for *Mycoplasma* contamination by Hoechst 33258 staining (20).

Tumor Fragments

The MX-1 breast carcinoma tumor fragments were originally obtained from the Frederick Research Tumor Repository and maintained by passage in NCr mice.

---

[3] W. Kemnitzer et al. Discovery of 4-aryl-4*H*-chromenes as a new series of apoptosis inducers using a cell- and caspase-based high throughput screening assay; structure-activity relationships of the 4-aryl group. J Med Chem. In press 2004.

Animals

Athymic (Crl:CD-1-*nu*Br) and severe combined immunodeficient [Crl:Icr:Ha(ICR)-scid] mice 6 to 8 weeks old were purchased from Charles Rivers Laboratories (St-Constant, Quebec, Canada). Tac:Cr;(NCr)-Hfh11*nu* (NCr) mice 6 to 8 weeks old were purchased from Taconic Farms (Germantown, NY). Animals were maintained under specific pathogen-free conditions and had access to sterile food and water *ad libitum*. All animal studies were done in the animal facility at Shire BioChem with the prior approval of the local Institutional Animal Care Committee and in agreement with the guidelines provided by the Canadian Council for Animal Care.

Pharmacokinetic Profiling

The six compounds under evaluation were given i.v. at a dose of 10 mg/kg to CD-1 male mice (*n* = 30 mice, per compound). Blood was collected into EDTA (final concentration, 2 mg/mL)–containing tubes by cardiac puncture at 2, 5, 15, 30, 45, 60, 90, 120, 180, and 240 minutes following compound administration. Samples were centrifuged at $10,000 \times g$ for 10 minutes and plasma samples were collected and stored at −20C until use. Mouse plasma (100 μL) was mixed with 50 μL internal standard and diluted with deionized water (900 μL). The mixture (∼1 mL) was loaded onto Oasis HLB 30-mg 96-well solid-phase extraction plate (Waters Corp., Milford, PA). After sequential washes with deionized water (1 mL) and 20% methanol (1 mL), the sample and the internal standard were eluted with acetonitrile (1 mL) and then evaporated to dryness under a gentle stream of nitrogen. The residues were reconstituted with 50% methanol (100 μL) in water and aliquots (10 μL) were analyzed by tandem liquid chromatography/mass spectrometry. The chromatography was achieved on a Luna C18 column (50 × 2 mm, 5 μm, Phenomenix, Torrance, CA) with a 5-minute elution gradient of acetonitrile (20–80%) in ammonium formate (10 mmol/L). The flow rate was 0.25 mL/min and total run time was at 12 minutes. Quantitation was done on a tandem liquid chromatography/mass spectrometry (TSQ7000, ThermoFinnigan, San Jose, CA) equipped with APCI source. Standard curve in mouse plasma ranged from 5 to 5,000 ng/mL, with minimum seven calibration points and three levels of quality controls.

Plasma concentration-time data were analyzed by non-compartmental linear pharmacokinetic methods using Kinetica (Innaphase, Philadelphia, PA). Maximum serum concentrations (C_{max}) were read directly from the experimental data, with t_{max} defined as the time of the first measurement (2 minutes). The terminal phase rate constants (k) were estimated using least squares regression analysis of the serum concentration-time data obtained during the terminal log-linear phase. The terminal half-life ($t_{1/2}$) was calculated by the equation $0.693/k$. The area under the serum concentration-time curve from time 0 to 240 minutes was estimated using linear trapezoidal approximation and was extrapolated to infinity according to the formula: $AUC_{(0 \rightarrow \infty)} = C_{last}/k$, where C_{last} is the

estimated concentration at time t_{last} = 240 minutes. Clearance was calculated as dose/AUC$_{(0 \to \infty)}$ and Vss was estimated as dose $\times$ AUMC/AUC^2, where AUMC is the area under the first moment curve (21).

Toxicity Studies

Toxicity profile of each tested compound was assessed after a single dose treatment or either a single or a twice daily treatment repeated for 5 consecutive days. A 14-day observation period followed the treatment period. CD-1 male mice (6–10 mice per dose) were given by a slow bolus injection at a constant volume of 10 mL/kg through the caudal vein while restrained in a plexiglass retainer tube. To monitor the general health condition and drug-associated toxicity, mice were weighed at least twice weekly and inspected daily for clinical abnormalities. The animals were euthanized under isoflurane anesthesia and blood was collected by cardiac puncture. The collected blood was immediately distributed into EDTA-containing tubes (hematology samples) or clotting gel–containing tubes (clinical chemistry samples) and sent for analysis at Cirion Biopharma, Inc. (Laval, Quebec, Canada). Macroscopic necropsies were done at 24 hours post-treatment (single dose) or after the last treatment (5-day repeat treatment) and again at the end of the 14-day observation period. Right kidney, liver, spleen, and thymus were weighed.

The MTD was estimated as the dose that resulted in ≤20% of body weight loss compared with the animal weight at the beginning of the treatment, <10% death rate, reversible observed clinical signs and hematology/clinical chemistry changes, and no visible macroscopic tissue changes at the end of the observation period. A drug dose was considered toxic if animals lost ≥20% of their initial body weight or if there was >10% lethality when applying humanized end points as described by the Canadian Council for Animal Care. The mice were prematurely euthanized when the MTD criteria were crossed or the established humanized end points as described by the Canadian Council for Animal Care were reached.

Tumor Necrosis and Vascular Dysfunction

Necrosis was assessed by light microscopy at 40× magnification. MDA-MB-435 tumor-bearing mice were injected with single doses of compounds at different concentrations as indicated. Tumors were excised 24 hours later and rapidly snap frozen in CryoMatrix (Cryomatrix, Pittsburgh, PA). Sections (6 μm) were prepared and stained with Gomori (Sigma Chemical Co., St. Louis, MO). The level of necrosis was scored visually according to the following scale: 1, 0-10% necrosis; 2, 11-20% necrosis; . . .; 10, 91-100% necrosis.

Functional vasculature was assessed as described previously (22). Hoechst 33342 (10 mg/kg) was injected into the tail vein of MDA-MB-435 tumor-bearing mice followed by a single bolus injection of vehicle, MX-116407 (10, 20, or 40 mg/kg), or CA4P (150 mg/kg). Four hours later, a second dye, DiOC$_7$(3), was injected; 2 minutes after injection, the mice were euthanized and tumors were rapidly removed, embedded in a tissue holder, and immediately frozen in liquid N_2 for sectioning. Perfused blood vessels in the tumor could be visualized by the surrounding halo of fluorescent Hoechst 33342– and/or DiOC$_7$(3)-labeled endothelial cells. The two dyes have different excitation and emission spectra, which allow separate detection. This method provides an estimate of the relative degree of perfused tumor vasculature. For each tumor, an average percentage image area was calculated. A total of three mice were imaged in each group.

Antitumor Efficacy Studies

Female severe combined immunodeficient mice were injected s.c. with 2×10^6 MDA-MB-435 cells. Tumor-bearing animals were randomized (10 mice per group) and treatment was started when tumor volumes reached 50 to 100 mm^3 (day 20). Doses and administration schedules are described in Table 1.

Female NCr mice were implanted s.c. by trocar in the right axillary area with MX1 tumor fragments (average, 2 mm^3). Tumor-bearing animals were randomized (9 mice per group) and treatment was started when the average tumor volumes reached ~150 mm^3. MX-76747, MX-116214, and MX-116407 were given i.v. at 10, 15, or 45 mg/kg, respectively, daily for 5 consecutive days (days 13-17). Mice were allowed a 2-day rest period and treated for another sequence (days 20-24). ZD6126 was given i.p. at 100 mg/kg following the same schedule.

Female athymic CD-1 (*nu/nu*) mice were injected s.c. with 2×10^6 Calu-6 cells in 50% Matrigel. Administration of compounds or vehicle began at day 24 when the average tumor size reached ~250 mm^3. Tumor-bearing animals were randomized (10 per group) prior to treatment. MX-76747, MX-116214, and MX-116407 were given i.v. at 10, 15, or 45 mg/kg, respectively, daily for 5 consecutive days

Table 1. Pharmacokinetic variables of selected compounds in mice after a single i. v. dose of 10 mg/kg

Compounds	MX-58151	MX-58276	MX-76747	MX-126303	MX-116214	MX-116407
C_{max} (μg/mL) at 2 min	26.5	28.9	26.3	12.3	19.4	10.0
AUC (μg × min/mL)	341.5	581.4	271.6	159.6	998.4	421.5
$t_{1/2}$ (min)	42.1	43.2	33.3	70.8	69.9	39.3
Clearance (mL/min)	0.69	0.43	0.81	1.4	0.25	0.62
Vss (mL)	20.3	11.7	11.5	50.8	20.6	34.9

(days 24–28). ZD6126 was given i.p. at 100 mg/kg on days 24 to 28. In the combination studies, a single dose of 4 mg/kg cisplatin was given i.p. 24 hours prior to treatment with MX-116407.

Tumor measurements taken by electronic calipers twice weekly were converted to tumor volumes (in mm^3) using the standard formula: width^2 × length × 0.52 (23). Compound efficacy was assessed once the tumors in the control group had reached at least five times their original volume (500% growth) by percentage of treated versus control (% T/C) defined as the (mean treated tumor volume) / (mean control tumor volume) × 100. A % T/C value of <42 was considered effective (24, 25). Tumor growth inhibition (TGI) was calculated by subtracting the % T/C from 100%. Tumor growth delay (TGD) was determined as the time delay necessary to double the mean tumor volume (starting from day 1 of treatment) in treated versus control animals. Statistical analysis was done by ANOVA or by Student's *t* test. Differences were considered to be significant at $P < 0.05$.

Results

Pharmacokinetics

The plasma concentration-time profiles and pharmacokinetic variables of MX-58151, MX-58276, MX-76747, MX-116214, MX-116407, and MX-126303 after single i.v. doses of 10 mg/kg are shown in Fig. 1 and Table 1, respectively. The clearance of the six compounds varied ~5-fold. MX-126303 was cleared at a rate close to the mouse liver blood flow (1.4 versus 1.8 mL/min; ref. 26), which resulted in one of the lowest measured C_{max} at 2 minutes (12.3 μg/mL) and lowest exposure (159.6 μg × min/mL) compared with the other five drug candidates. In contrast, MX-116214 was characterized by the slowest clearance of this series (0.25 mL/min) and had the greatest exposure (998.4 μg × min/mL), resulting in plasma concentrations in the micromolar range up to 4 hours. Despite their differences in clearance,

these two compounds had the longest terminal half-lives (~70 minutes), suggesting that the tissue distribution is greater for MX-126303 than for MX-116214. The other compounds were characterized by intermediate plasma clearances and terminal elimination half-lives of ~40 minutes. Highest initial concentrations were achieved by MX-58151, MX-58276 and MX-76747 (26–29 μg/mL).

Induction of Tumor Necrosis and Tumor Vascular Disruption

Table 2 summarizes the toxicity profiles as well as the dose-response data of the six lead compounds for induction of tumor necrosis after i.v. administration to mice bearing the human breast (MDA-MB-435) tumor xenograft. MX-58151 and MX-58276 induced extensive necrosis (80–90%) after a single administration of 25 and 110 mg/kg, respectively. These doses were well tolerated when given as a single injection but resulted in weight loss and reversible toxicity when given for 5 consecutive days. For MX-76747, MX-116214, MX-116407, and MX-126303, MTD was determined following a single bolus injection and a 2- to 6-fold toxicity difference was observed between acute and repeated dosing. MX-116214 and MX-126303 induced extensive tumor necrosis (80–90%) but only at doses close to their respective MTD. On the other hand, MX-76747 and MX-116407 were more effective, causing substantial tumor necrosis (60–80%) at doses of one-fourth to one-sixth of their respective MTDs. This compares well with ZD6126 in this tumor model, where we observed significant tumor necrosis (60–80%) at doses approaching one-third to one-fourth of its MTD (Table 1). In our hands, ZD6126 was found to be toxic following a bolus injection of 300 mg/kg (causing hypothermia, respiratory difficulties, and eventually death) but was well tolerated at 150 mg/kg (mild loss of body weight, reduction of spleen weight, decrease in activity, and matted fur).

MX-116407 was further evaluated by examining the regrowth of the MDA-MB-435 tumor following a single bolus administration. Twenty-four hours after treatment,
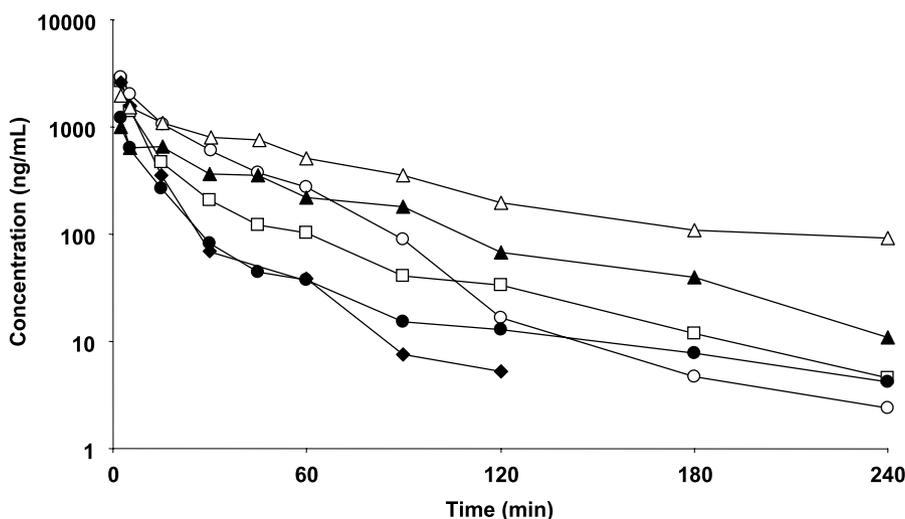

Figure 1. Plasma concentration-time curves of selected compounds. The pharmacokinetics of MX-58151 (□), MX-58276 (○), MX-76747 (◆), MX-116214 (△), MX-116407 (▲), and MX-126303 (●) were evaluated in male CD-1 mice ($n = 3$ per time point). A single dose of each different compound was given i.v. at 10 mg/kg. Plasma was collected by cardiac puncture at 2, 5, 15, 30, 60, 90, 120, 180, and 240 minutes following compound administration.

Table 2. Induction of tumor necrosis in the human breast (MDA-MB-435) tumor xenograft 24 hours postdosing

Compounds	Dose (mg/kg)	MTD* (mg/kg)	Median necrosis score[†]
ZD6126	140	Single i.p. treatment between 150 and 300	8.3
	100		8
	50		6.3
	25		4.7
MX-58151	25	qd × 5 = 20	9.8
	8		
	4		3.3
MX-58276	110	b.i.d. × 5 = >90	8.3
	75		
	40		4.6
	20		
MX-76747	60	Single i.v. dose = 60 b.i.d. × 5 = 10	8.2
	40		8.2
	20		6.5
	10		5
MX-116214	25	Single i.v. dose = 25 qd × 5 = 15	9.3
	12.5		5.3
	6.3		3.3
	2.5		3
MX-116407	100	Single i.v. dose = 100 qd × 5 = >40	9
	75		7
	50		6.7
	25		8
MX-126303	2.5	Single i.v. dose = 2.5 b.i.d. × 5 = 1	6.3
	0.8		5.7
	0.4		

*The MTD is the dose at which we observed body weight loss (<20%), pale livers, pale kidneys, thrombocytopenia, and diarrhea. These symptoms were observed after the treatment period but were no longer present at the 14-day observation period. qd, single daily dose repeated over 5 consecutive days; b.i.d., twice daily dose repeated over 5 consecutive days.
[†]Necrosis index was determined following Gomori staining and scoring with 1 representing 10% necrosis and 10 representing complete (100%) necrosis. Three animals were used per time point.

although 90% of the tumor were necrotic (Fig. 2B; Table 2), we did not measure tumor reduction (Fig. 2A). This is likely to be due to edema resulting from an inflammatory reaction related to the extensive tumor necrosis. The tumor volume started to decrease thereafter, and by 7 days after treatment, we observed a 25% growth reduction (Fig. 2A). Between days 7 and 14 post-treatment, the tumor volume gradually increased. By day 14, the tumor had repopulated itself with marginal necrosis observed at the center of the tumor (Fig. 2C).

The observed rapid and extensive tumor necrosis is indicative of vascular disruption in the tumor. We have also examined the level of functional tumor vasculature after compound treatment by a double fluorescent dye staining

method (22). The DNA-binding fluorescent Hoechst 33342 is first given to allow staining of tumor blood vessels followed by compound administration. Four hours later, a second dye was given and tumors were quickly excised,
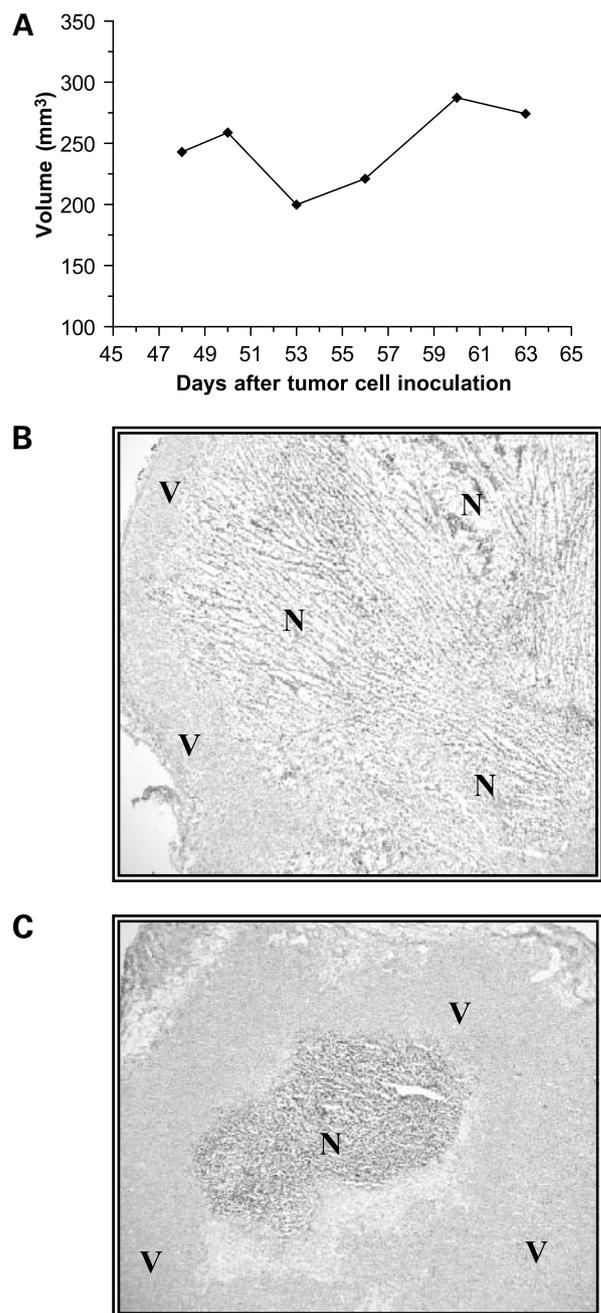

Figure 2. Regrowth of MDA-MB-435 tumors after a single dose of MX-116407. Twelve mice bearing MDA-MB-435 tumor xenografts were treated with a single i.v. bolus dose of MX-116407 (100 mg/kg) when tumors reached an average volume of 250 mm^3 (*day 49*). **A,** tumors were measured twice weekly and on days 1, 4, 7, and 14 after treatment with MX-116407. Three mice were sacrificed for tumor necrosis evaluation. **B,** Gomori staining 24 hours after treatment (×40). **C,** Gomori staining 14 days after treatment (×40). Representative necrotic (*N*) and viable (*V*) regions are identified. Regrowth seems to originate from the tumor rim.

frozen, and then sectioned for examination. The sections were examined for the amount of fluorescence from the two distinguishable dyes. The fluorescent image area for each dye was determined and the results are expressed as the percentage of the second dye over the first dye (Fig. 3). The vehicle showed very little effect on the extent of dye label between the two dyes. MX-116407 showed a dose dependence of reducing the amount of the second dye, as did CA4P which serves as a positive control, demonstrating that it is acting as a vascular disrupting agent.

Antitumor Efficacy Studies

To determine if the antivascular activity of these compounds was sufficient to result in TGD, the compounds were evaluated for antitumor activity in the same tumor xenograft model. Because the MDA-MB-435 tumor grows slowly, having a doubling time of 12 days, and the half-life of the compounds varied from 30 to 70 minutes, the treatment regimens were daily or twice daily for 5 consecutive days repeated for up to 3 weeks. MX-58151, MX-58276, and MX-126303 resulted in TGDs of 8, 4, and 6 days and % T/Cs of 65, 75, and 75, respectively (Table 3). These values indicated marginal antitumor activity for these compounds in this model. For MX-58151 and MX-58276, the marginal antitumor activity could be due to the shorter period of treatment (5 consecutive days instead of up to 3 weeks). On the other hand, MX-76747, MX-116214, and MX-116407 were more potent, resulting in TGDs of 12, 15, and 16 days and % T/Cs of 58, 55, and 43, respectively (Table 3). Because MX-76747, MX-116214, and MX-116407 showed good antitumor activity, they were evaluated in two other human xenografts and compared with ZD6126 using the same schedule of administration.
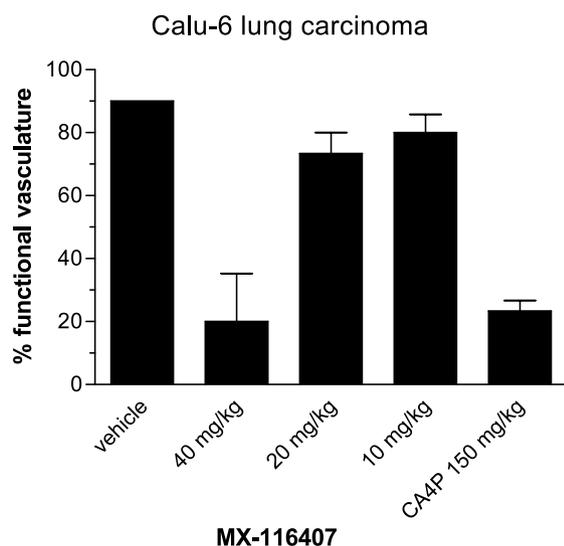
Table 3. Antitumor efficacy in the breast (MDA-MB-435) human tumor xenograft

Compounds	Dose/schedule	TGD (d)	% T/C
ZD6126	200 mg/kg q6d × 3	8	68
MX-58151	10 mg/kg b.i.d. × 5 d	8	65
MX-58276	40 mg/kg b.i.d. × 5 d	4	75
MX-76747	10 mg/kg (q1d × 5) 3 wk	12	58
MX-116214	15 mg/kg (q1d × 5) 3 wk	15	55
MX-116407	45 mg/kg (q1d × 5) 3 wk	16	43
MX-126303	1 mg/kg (q1d × 5) 3 wk	6	75

In the human breast MX1 tumor xenograft, compounds were given when the tumor fragments had reached ∼150 mm³ (effect of compounds on tumor growth and body weight is shown in Fig. 4). Whereas the average tumor size increased from 147 to 1,879 mm³ in the control group (representing a 12.8-fold increase), administration of MX-76747, MX-116214, and MX-116407 led to increases of 1.9-, 2.4-, and 0.9-fold, respectively. In the ZD6126-treated groups, the average tumor volume increased 3-fold. At
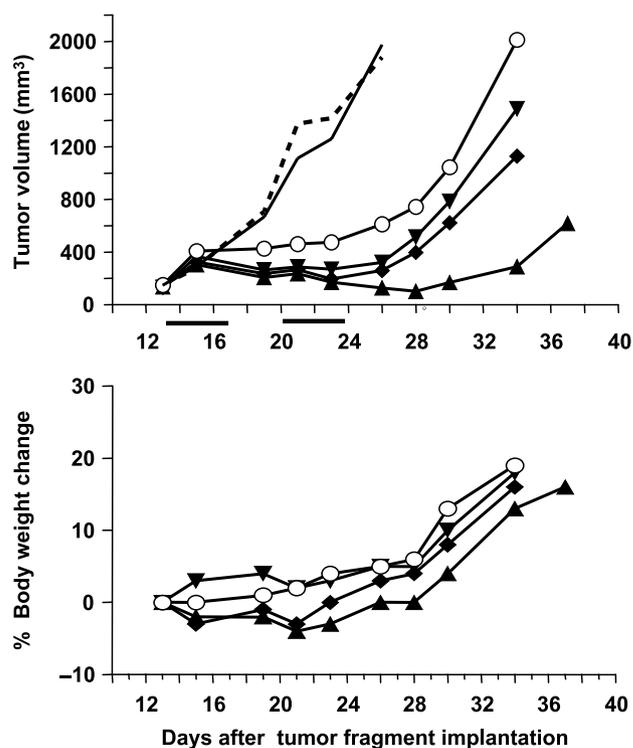

Figure 3. Functional vasculature determination following single dose of MX-116407. Perfused vasculature in the Calu-6 tumor was assessed by a double fluorescent dye staining procedure as described in Materials and Methods. Vehicle and CA4P were used as negative and positive controls, respectively. *Columns,* mean of three animals per group; *bars,* SD.

Figure 4. Activity of selected compounds against the human breast (MX1) tumor xenograft. MX1 human breast fragments were implanted s.c. by trocar in *nu/nu* female mice. Treatment was initiated when the primary tumor reached a size of ∼150 mm³ (*day 13*). MX-76747 (10 mg/kg, ♦), MX-116214 (15 mg/kg, ▼), and MX-116407 (45 mg/kg, ▲) were given i.v. on *days 13–17* and *days 20–24*. ZD6126 (100 mg/kg, ○) was given i.p. on the same days. Saline control group (*solid line*); Cremophor/ethanol/dextrose control group (*dashed line*). *Solid horizontal bar,* treatment period.

the time vehicle groups were terminated, we observed TGIs of 75% to 91% for the MX compounds ($P < 0.001$) compared with a TGI of 64% ($P = 0.03$) for ZD6126. Moreover, tumor regression was observed with MX-116407. Tumor growth resumed after the termination of treatment, but TGDs of over 10 days were observed (Fig. 4, *top*) at doses that were well tolerated as indicated by no significant body weight loss (Fig. 4, *bottom*).

In the human lung Calu-6 xenograft, compounds were given when the tumor fragments had reached an average size of 250 mm^3 (24 days after tumor cell inoculation). MX-76747, MX-116214, MX-116407, and ZD6126 were given daily for 5 consecutive days at doses near but below their respective MTDs (Fig. 5). MX-76747 and MX-116214 did not show significant antitumor activity in this model resulting in TGIs of 10% and 28% at day 42, time at which the control group had to be sacrificed ($P > 0.5$). On the other hand, MX-116407 showed highly significant antitumor activity with tumor regressions occurring from days 28 to 45 and TGI of 86% at day 42 ($P = 0.01$). ZD6126 had moderate antitumor activity in this model with tumor stasis occurring from days 28 to 34 and TGI of 47% at day 42 ($P = 0.3$).

When MX-116407 was examined in combination with a moderately active dose of cisplatin (4 mg/kg i.p. given 24 hours before MX-116407), we observed significant tumor regression occurring from day 28 in all 10 treated mice (Fig. 6A), with four animals remaining tumor free at day 104 when the study was terminated, which was 85 days after the last drug dose. At day 42, the time at which animals from the control group had to be sacrificed, the average % T/C value was 13 (Fig. 6B). Body weight losses in the MX-116407-treated and MX-116407/cisplatin–treated groups were <10%.
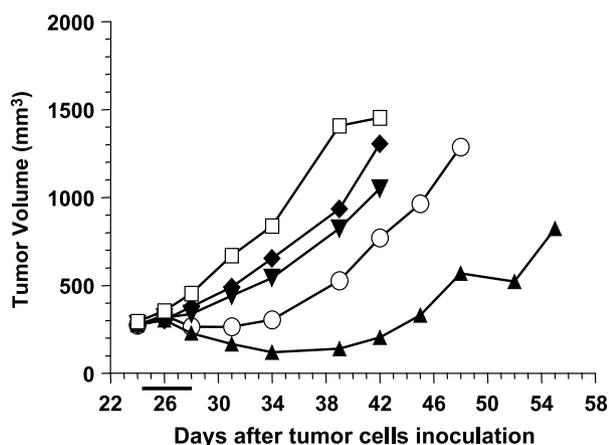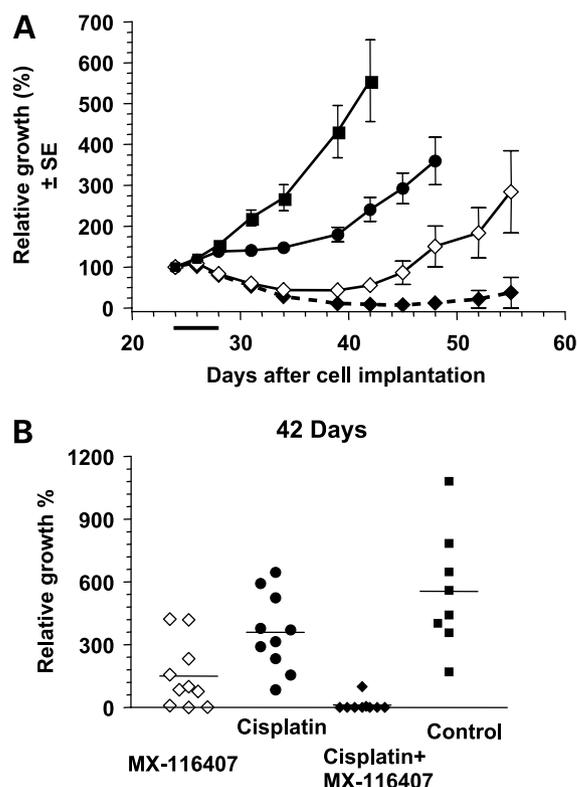
Figure 6. Growth of Calu-6 human tumor xenografts after treatment with MX-116407 in combination with cisplatin. Treatment was initiated when tumors reached an average size of 250 mm^3 (*day 24*). Cisplatin was given daily at 4 mg/kg i.p. (●) 1 day prior to MX-116407. MX-116407 was given daily for 5 days at 45 mg/kg alone (◇) or in combination with cisplatin (◆). Vehicle control group (Cremophor/ethanol/saline) was dosed daily for 5 days (■). **A,** tumor growth results are expressed as a percentage of growth in relation to the size of each tumor on the day of first treatment (this value was set as 100% and tumor growth is reported in percentage). **B,** relative tumor volumes of all the animals from the different treatment groups are compared at *day 42*, after which time animals from the control group had to be sacrificed due to tumor burden. *Solid horizontal bar,* treatment period for MX-116407 and vehicle.

Discussion

We have reported previously that a group of 4-aryl-4*H*-chromenes (i.e., MX-58151, MX-58276, MX-76747, MX-116214, MX-116407, and MX-126303) had potent *in vitro* cytotoxic activity, bound to tubulin at the colchicine site, caused a G$_2$-M-phase cell arrest, and induced apoptosis (4). The compounds also had an effect on endothelial cell function as shown by their ability to disrupt preformed capillary tubes in the three-dimensional Matrigel tubule formation assay (4). This property, suggestive of antiangiogenic and antivascular activities (17, 27), led us to evaluate the antitumor activity of this group of compounds.

Tubulin-binding agents are known to have antivascular activity, but for most compounds, this effect is observed at or close to the MTD (5). However, the newer generation of tubulin-interacting agents, such as CA4P and ZD6126, have shown a selective effect against tumor vasculature at doses around one-third (28) to one-tenth (29, 30) of their

Figure 5. *In vivo* antitumor activity of selected compounds against the human lung (Calu-6) tumor xenograft. BALB/c female nude mice 6–8 weeks old were injected s.c. with 2×10^6 Calu-6 cells (day 0). Treatment was initiated when the primary tumor reached a size of ~250 mm^3 (*day 24*). MX-76747 (10 mg/kg, ◆), MX-116214 (15 mg/kg, ▼), and MX-116407 (45 mg/kg, ▲) were given i.v. on *days 24–28*. ZD6126 (100 mg/kg, ○) was given i.p. on the same days. Vehicle control (Cremophor/ethanol/saline) group (□). *Solid horizontal bar,* treatment period.

respective MTDs. The six compounds profiled in this study all induced extensive tumor necrosis. Within 24 hours of administration, the entire center of the tumor was necrotic with a thin viable rim of tumor cells surviving at the periphery. This pattern of central necrosis with a thin viable rim of tumor cells was first reported with CA4P (30) and is consistent with vasculature targeting agents (18, 31–33). However, when the dose required to induce significant tumor necrosis was compared with the dose that caused significant but reversible toxicities, it became evident that some compounds were more effective than others.

Also observed with this series of compounds was that the compounds with the most potent antivascular effects were not the most potent *in vitro* (4). Indeed, although MX-126303 had the best *in vitro* cytotoxic activity, it induced tumor necrosis at levels close to its MTD, suggesting that its toxicity is linked with its effect on tubulin inhibition rather than targeting selectively endothelial cells. The antivascular activity of MX-126303 is reminiscent of other tubulin-binding agents, such as colchicine and vinblastine, which have vascular-damaging activity only at their MTDs. However, its pharmacokinetic profile is similar to classic antivascular agents such as ZD6126 and CA4P, which have short plasma half-lives (29, 34). On the other hand, MX-116407, while less cytotoxic than MX-126303 *in vitro*, had more tumor-selective antivascular activity. We observed 80% tumor necrosis at 25 mg/kg, corresponding to one-fourth of its MTD. This may be related to the differences in pharmacokinetic profile. Although both MX-116407 and MX-126303 have rapid distribution phases, resulting in maximum concentrations at the earliest time point evaluated (10 and 12.3 μg/mL, respectively), their clearance rates were quite different, varying by 2.4-fold. This results in a 8-fold difference in concentration after 45 minutes (3.5 versus 0.44 μg/mL for MX-116407 and MX-126303, respectively; Fig. 1). A rapid distribution coupled with a slow clearance is thus likely to be important for good antitumor activity.

A second explanation might relate to our finding that apoptosis induction following a 3-hour treatment with MX-126303 is irreversible after drug washout, whereas induction of apoptosis following MX-116407 treatment is reversible (4). This may suggest that MX-116407 and MX-126303 have different tubulin-binding kinetics, leading to differences in pharmacologic profile. Indeed, the improved therapeutic index observed with CA4P compared with colchicine has been correlated to their differences in the on/off rate of binding to tubulin (11, 17, 35), leading to the hypothesis that a successful vascular targeting agent would have reversible binding kinetics and relatively rapid clearance *in vivo* (19).

The vascular targeting activity of this novel series of compounds, suggested by the induction of tumor necrosis, led us to investigate their antitumor potential. Whereas treatment of mice bearing MDA-MB-435 tumor xenografts with MX-58151, MX-58276, and MX-126303 resulted in poor antitumor activity with % T/Cs of 65, 75, and 75, respectively, MX-76747, MX-116214, and MX-116407 resulted in moderate antitumor activity with % T/Cs of

58, 55, and 43, respectively. According to National Cancer Institute criteria, compounds resulting in % T/C values of ≤42 are considered to have antitumor activity (24). The moderate antitumor activity is likely a result of regrowth of the tumor originating from the viable rim of tumor cells remaining after the treatment. We have observed that the MDA-MB-435 tumors have repopulated spontaneously 14 days after the cessation of treatment, although % T/C values were calculated at day 50, 10 days after cessation of treatment. We have further evaluated MX-76747, MX-116214, and MX-116407 in other human tumor xenograft models. In the human breast (MX-1) tumor xenograft, all three compounds showed significant antitumor activity with % T/Cs ranging between 0.7 and 17. In the human lung (Calu-6) tumor xenograft, MX-116407 was highly active, producing tumor regressions in all 10 animals. Moreover, MX-116407 significantly enhanced the antitumor activity of cisplatin, producing tumor-free animals in a significant number (4 of 10) of cases at time of sacrifice.

In summary, we have identified 2-amino-4-(3-bromo-4,5-dimethoxy-phenyl)-3-cyano-4*H*-chromenes as a novel series of vascular targeting agents with promising antitumor activity. Our encouraging results with MX-116407 strongly support its continued development as a novel anticancer agent for human use.

References

1. Cai SX, Nguyen B, Jia S, et al. Discovery of substituted *N*-phenyl nicotinamides as potent inducers of apoptosis using a cell- and caspase-based high throughput screening assay. J Med Chem 2003;46:2474–81.

2. Cai SX, Zhang HZ, Guastella J, et al. Design and synthesis of rhodamine 110 derivative and caspase-3 substrate for enzyme and cell-based fluorescent assay. Bioorg Med Chem Lett 2001;11:39–42.

3. Zhang HZ, Kasibhatla S, Wang Y, et al. Discovery, characterization and SAR of gambogic acid as a potent apoptosis inducer by a HTS assay. Bioorg Med Chem 2004;12:309–17.

4. Kasibhatla S, Gourdeau H, Meerovitch K, et al. Discovery and mechanism of action of a novel series of apoptosis inducers with potential vascular targeting activity. Mol Cancer Ther 2004;3:1365–73.

5. Ben-Ze'ev A. Cell shape, the complex cellular networks, and gene expression. Cytoskeletal protein genes as a model system. Cell Muscle Motil 1985;6:23–53.

6. Bernal SD, Stahel RA. Cytoskeleton-associated proteins: their role as cellular integrators in the neoplastic process. Crit Rev Oncol Hematol 1985;3:191–204.

7. Thyberg J, Moskalewski S. Microtubules and the organization of the Golgi complex. Exp Cell Res 1985;159:1–16.

8. Rowinsky E, Donehower R, editors. Antimicrotubule agents. Philadelphia: Lippincott-Raven Publishers; 1997. p. 467–83.

9. Rowinsky EK. The development and clinical utility of the taxane class of antimicrotubule chemotherapy agents. Annu Rev Med 1997;48:353–74.

10. Jordan MA, Wilson L. Microtubules and actin filaments: dynamic targets for cancer chemotherapy. Curr Opin Cell Biol 1998;10:123–30.

11. Jordan MA. Mechanism of action of antitumor drugs that interact with microtubules and tubulin. Curr Med Chem Anti-Canc Agents 2002;2:1–17.

12. Hadfield JA, Ducki S, Hirst N, McGown AT. Tubulin and microtubules as targets for anticancer drugs. Prog Cell Cycle Res 2003;5:309–25.

13. Dumontet C, Sikic BI. Mechanisms of action of and resistance to antitubulin agents: microtubule dynamics, drug transport, and cell death. J Clin Oncol 1999;17:1061 – 70.

14. Li Q, Sham H. Discovery and development of antimitotic agents that inhibit tubulin polymerization for the treatment of cancer. J Clin Oncol 2002;17:1061 – 70.

15. Baguley BC, Holdaway KM, Thomsen LL, Zhuang L, Zwi LJ. Inhibition of growth of colon 38 adenocarcinoma by vinblastine and colchicine: evidence for a vascular mechanism. Eur J Cancer 1991;27:482 – 7.

16. Marx M. Small-molecule, tubulin-binding compounds as vascular targeting agents. Expert Opin Ther Patents 2002;12:769 – 76.

17. Griggs J, Metcalfe JC, Hesketh R. Targeting tumor vasculature: the development of combretastatin A4. Lancet Oncol 2001;2:82 – 7.

18. Micheletti G, Poli M, Borsotti P, et al. Vascular-targeting activity of ZD6126, a novel tubulin-binding agent. Cancer Res 2003;63:1534 – 7.

19. Davis PD, Dougherty GJ, Blakey DC, et al. ZD6126: a novel vascular-targeting agent that causes selective destruction of tumor vasculature. Cancer Res 2002;62:7247 – 53.

20. Chen TR. *In situ* detection of *Mycoplasma* contamination in cell cultures by fluorescent Hoechst 33258 stain. Exp Cell Res 1977; 104:255 – 62.

21. Rowland M, Tozer TN. In: Rowland M, Tozer TN, editors. Clinical pharmacokinetics: concepts and application. Philadelphia: Lae & Febiger; 1989. p. 9 – 100.

22. Tufto I, Rofstad EK. Transient perfusion in human melanoma xenografts. Br J Cancer 1995;71:789 – 93.

23. Tomayko MM, Reynolds CP. Determination of subcutaneous tumor size in athymic (nude) mice. Cancer Chemother Pharmacol 1989;24:148 – 54.

24. Plowman J, Dykes D, Hollingshead, M, Simpson-Herren L, Alley MC. In: Teicher B, editor. Anticancer drug development guide: preclinical screening, clinical trials, and approval. Totowa (NJ): Humana Press Inc; 1997. p. 101 – 25.

25. Johnson JI, Decker S, Zaharevitz D, et al. Relationships between drug activity in NCI preclinical *in vitro* and *in vivo* models and early clinical trials. Br J Cancer 2001;84:1424 – 31.

26. Davies B, Morris T. Physiological parameters in laboratory animals and humans. Pharm Res 1993;10:1093 – 5.

27. Hotchkiss KA, Ashton AW, Mahmood R, et al. Inhibition of endothelial cell function *in vitro* and angiogenesis *in vivo* by docetaxel (Taxotere): association with impaired repositioning of the microtubule organizing center. Mol Cancer Ther 2002;1:1191 – 200.

28. Grosios K, Holwell SE, McGown AT, Pettit GR, Bibby MC. *In vivo* and *in vitro* evaluation of combretastatin A-4 and its sodium phosphate prodrug. Br J Cancer 1999;81:1318 – 27.

29. Blakey DC, Westwood FR, Walker M, et al. Antitumor activity of the novel vascular targeting agent ZD6126 in a panel of tumor models. Clin Cancer Res 2002;8:1974 – 83.

30. Dark GG, Hill SA, Prise VE, et al. Combretastatin A-4, an agent that displays potent and selective toxicity toward tumor vasculature. Cancer Res 1997;57:1829 – 34.

31. Nihei Y, Suzuki M, Okano A, et al. Evaluation of antivascular and antimitotic effects of tubulin binding agents in solid tumor therapy. Jpn J Cancer Res 1999;90:1387 – 95.

32. Otani M, Natsume T, Watanabe JI, et al. TZT-1027, an antimicrotu-bule agent, attacks tumor vasculature and induces tumor cell death. Jpn J Cancer Res 2000;91:837 – 44.

33. Nilsson F, Kosmehl H, Zardi L, Neri D. Targeted delivery of tissue factor to the ED-B domain of fibronectin, a marker of angiogenesis, mediates the infarction of solid tumors in mice. Cancer Res 2001;61:711 – 6.

34. Dowlati A, Robertson K, Cooney M, et al. A phase I pharmacokinetic and translational study of the novel vascular targeting agent combretastatin A-4 phosphate on a single-dose intravenous schedule in patients with advanced cancer. Cancer Res 2002;62:3408 – 16.

35. Lin CM, Ho HH, Pettit GR, Hamel E. Antimitotic natural products combretastatin A-4 and combretastatin A-2: studies on the mechanism of their inhibition of the binding of colchicine to tubulin. Biochemistry 1989;28:6984 – 91.

Molecular Cancer Therapeutics

Antivascular and antitumor evaluation of 2-amino-4-(3-bromo-4,5-dimethoxy-phenyl)-3-cyano-4 *H* -chromenes, a novel series of anticancer agents

Henriette Gourdeau, Lorraine Leblond, Bettina Hamelin, et al.

Updated version	Access the most recent version of this article at: http://mct.aacrjournals.org/content/3/11/1375

Cited articles	This article cites 29 articles, 8 of which you can access for free at: http://mct.aacrjournals.org/content/3/11/1375.full#ref-list-1

E-mail alerts	Sign up to receive free email-alerts related to this article or journal.
Reprints and Subscriptions	To order reprints of this article or to subscribe to the journal, contact the AACR Publications Department at pubs@aacr.org.
Permissions	To request permission to re-use all or part of this article, use this link http://mct.aacrjournals.org/content/3/11/1375. Click on "Request Permissions" which will take you to the Copyright Clearance Center's (CCC) Rightslink site.